The Cryosphere Discuss., 4, 2169–2199, 2010
www.the-cryosphere-discuss.net/4/2169/2010/
doi:10.5194/tcd-4-2169-2010

The Cryosphere Discussions

Thermal structure and drainage system of a small valley glacier (Tellbreen, Svalbard), investigated by Ground Penetrating Radar

K. Bælum[1] **and D. I. Benn**[1,2]

[1]Department of Geology, University Centre in Svalbard (UNIS), Longyearbyen, Norway
[2]School of Geography and Geosciences, University of St. Andrews, UK

Received: 13 October 2010 – Accepted: 13 October 2010 – Published: 21 October 2010

Correspondence to: K. Bælum (karolineb@unis.no)

Published by Copernicus Publications on behalf of the European Geosciences Union.

Thermal structure and drainage system of a small valley glacier

K. Bælum and D. I. Benn

Abstract

Proglacial icings accumulate in front of many High Arctic glaciers during the winter months, as water escapes from englacial or subglacial storage. Such icings have been interpreted as evidence for warm-based subglacial conditions, but several are now known to occur in front of cold-based glaciers. In this study, we investigate the drainage system of Tellbreen, a 3.5 km long cold-based polythermal glacier in central Spitsbergen, where a large proglacial icing develops each winter, to determine the location and geometry of storage elements. DEMs of the glacier surface and bed were constructed using maps, differential GPS and GPR. Patterns of surface lowering indicate that the glacier has a long-term mass balance of -0.6 ± 0.2 m/year. Englacial and subglacial drainage channels were mapped using Ground penetrating radar (GPR), showing that Tellbreen has a diverse drainage system that is capable of storing, transporting and releasing water year round. In the upper part of the glacier, drainage is mainly via supraglacial channels. These transition downglacier into shallow englacial "cut and closure" channels, formed by the incision and closure of supraglacial channels. Below thin ice near the terminus, these channels reach the bed and contain stored water throughout the winter months. Even though the bed is below pressure-melting point, Tellbreen has a surface-fed, channelized subglacial drainage system, which allows significant storage and delayed discharge.

1 Introduction

Large icings (also known as naled ice) accumulate each winter in front of many glaciers in Svalbard. Although snow-melt can occur during brief periods of positive air temperature in winter (Humlum, 2003), this source of water is insufficient to explain either the volume or quasi-continuous accumulation of proglacial icings, and the out-flowing water most likely reflects the release of water from en- or subglacial storage. Traditionally the presence of large icings has been interpreted as evidence for warm-based polythermal

TCD
4, 2169–2199, 2010

conditions (Hagen, 2003), under which water can be produced subglacially throughout the year. Some studies have shown that icings also occur in front of glaciers which are predominantly or entirely cold-based (Hodgkins, 1997), although in such cases the location and distribution of stored water are poorly known.

There have been comparatively few investigations of drainage systems on predominantly cold based arctic glaciers with evident outflow of water in the winter season (Hodgkins, 1997; van Hoof, 2008; Temminghoff, 2009), and considerable uncertainty exists about the source, flowpath, and residence time of such water. In this study, we use GPR data to investigate the thermal characteristics, structure, and drainage system of Tellbreen, a small valley glacier in central Spitsbergen. Specifically, the aims of this paper are: (1) to determine the thermal regime of the glacier, particularly whether there are any areas of temperate ice, (2) to establish the location of stored water within and beneath the glacier, and its relationship with englacial and subglacial drainage channels, and (3) to determine changes in the area, volume and thickness of the glacier since the Little Ice Age, to provide a context for other data.

2 Setting

The Archipelago of Svalbard consists of all islands located between 74° and 80° N and 10° and 35° E. The climate is relatively mild and dry compared to other locations at similar latitudes, with an average annual air temperature of −6 °C and a mean annual precipitation of 400 mm in the central part of Spitsbergen, the main island (Engeset, 1999). Sixty percent of the land area is covered by glaciers (Hagen, 1993).

Tellbreen is a medium size, land terminating valley glacier situated at 78.13° N, 16.5° E in the centre of Spitsbergen (Fig. 1), 20 km northeast of the main settlement, Longyearbyen. It has not previously been the objective of scientific investigations. The glacier's basic properties (estimated from aerial photos from 1977) are listed in the Glacier Atlas of Svalbard and Jan Mayen (Hagen, 1993) (Table 1). The median elevation is 580 m a.s.l. which is very close to the mid point of the glacier (570 m a.s.l)

TCD
4, 2169–2199, 2010

indicating a simple hypsometry with an area to height ratio of close to one. The volume of the glacier is calculated from the ice covered area observed on the 1977 aerial photos (A) and the mean depth (D) which is estimated by

$$D = 33 \times ln\,A + 25. \text{ (Hagen, 1993).} \quad (1)$$

Tellbreen has a well defined catchment area, a single firn area and has experienced substantial retreat of the terminus since the LIA. A large icing and areas of open water occur every winter in front of the glacier terminus. We have observed open water in front of the glacier even at times when temperatures were below −20 °C, indicating release of stored englacial or subglacial water.

The geology of the area consists of sub-horizontal, poorly cemented and readily erodible fluvial and shallow marine sand- and siltstones of Cretaceous to Eocene age (Hjelle, 1993). There are no known faults directly under Tellbreen, but the major Billefjorden fault zone is found 10 km to the east. Further more there are several faults in the nearby De Geerdalen and under the Archowskifjellet (Dallmann, 1993). Several of the pingos in the area, such as the two in the De Geerdalen and the Innerhytta Pingo are found in connection with these fault lines (Ross, 2005).

Traditionally, it has been assumed that drainage on cold arctic glaciers is entirely supraglacial, because melt water is unable to penetrate cold ice (Hodkins, 1997). However, recent work has shown that two mechanisms can enable surface melt water to reach the interior, and sometimes the bed, of predominantly cold polythermal glaciers (Gulley et al., 2009a). First, incision of perennial surface melt water channels can form meandering englacial passages if their upper, abandoned levels become blocked by snow or ice, or closed by ice creep (Gulley et al., 2009b). Such "cut-and-closure" conduits commonly form in lateral positions due to the convex shape of the ablation area (e.g. Longyearbreen: Hansen, 2001; Humlum, 2005; Gulley et al., 2009b), although they can also occur close to the glacier centreline (e.g. Austre Brøggerbreen; Vatne, 2001). Cut-and-closure conduits can incise down to glacier beds and form subglacial channels in cold ice (e.g. Humlum et al., 2005; Gulley et al., 2009b), although channels

TCD
4, 2169–2199, 2010

below depths of ~20 m of ice are very susceptible to blockage, and water tends to be re-routed to shallower flow paths.

The second mechanism for routing surface melt water through cold ice is overdeepening of water-filled crevasses, or hydrofracturing (Boon and Sharp, 2002; Alley et al., 2005; van der Veen, 2008; Benn et al., 2009). Hydrofracturing can occur where ice under tensile deviatoric stress coincides with a sufficient water supply. This then allow surface-to-bed drainages (moulins) to develop on a seasonal basis, and enables the water to access deep, warm areas of glacier beds through great thicknesses of cold ice. On Tellbreen, the ice surface is mostly smooth with no major crevasse areas. Although some isolated extensional crevasses occur on the upper part of the north-west side of the glacier, and bergschrunds occur near its upper limit, we have found no evidence for surface-to-bed drainage by hydrofracturing on Tellbreen. Surface melt water follows well-defined supraglacial channels in the upper part of the glacier, with a shift to an arborescent system of partly englacial, 10–20 m deep, incised lateral channels in the lower part.

3 Methods

3.1 GPR

During the spring field seasons of 2004, 2005 and 2009 a total of 98 km of GPR lines were recorded on Tellbreen with about 50% being repetitive to detect changes in the glacier geometry. In 2010, a total of 26 km were recorded in a grid covering the lower third of the glacier. The equipment used in 2004–2005 was a PulsEKKO 100 radar triggered by an odometer wheel. The antennae were mounted on a wooden sledge perpendicular to the direction of movement with equidistant spacing of one antenna length between them. This was done to minimize line interferences from objects either side of the lines and to optimize the amount of energy transmitted directly into the ground (Annan, 1992) as the antenna radiation pattern is that of a half wavelength dipole (Daniels, 1996). A snow scooter was used to tow the sledge and carry the rest of the equipment. We used 50 and 100 MHz resistively damped dipolar antennae, with bandwidths equal to their centre frequency (Daniels 1996).

In 2009 and 2010, a Målå radar system with fixed, unshielded, 100 MHz antenna was used. The antennas were inline with an equidistant spacing of two antenna lengths between them. Since the antenna array is fixed in a Kevlar tube, this system does not allow for making a common mid point (CMP) survey. Velocities were therefore adopted from three CMP surveys recorded on nearby Longyearbreen (78.11° N, 15.3° E) in the spring of 2005. These give velocities of 0.16 ± 0.02 m/ns (Bælum, 2006) which is close to the theoretical values for clean dry ice 0.168 ± 0.003 m/ns (Petterson, 2003). A value of 0.17 m/ns was used for depth conversion of the GPR data from Tellbreen.

In 2005, 2009 and 2010 a Garmin Etrex legend GPS was used for positioning the radar lines. Kinematic DGPS measurements covering most of the glacier surface were collected in April of 2009. These measurements were used to model the 2009 surface. The accuracy given by the GPS was in most cases 5–10 m in the horizontal plane. Points with lesser accuracy were not used. The vertical accuracy was 3–8 m in 2009 when comparing the GPS to the DGPS measurements taken at the same location. A vertical error of 10m corresponds to 2–3% of the total heights in m a.s.l. The topographic maps of the area have contour interval of 50 m, so this error is negligible in respect to the topographic models presented.

3.2 Areal photographs and maps

The most resent aerial photographs of Tellbreen are the Norwegian Polar Institute 1:15 000 series from 1990 and 1995. For this investigation the pictures used were the S95 1226 and 1227 and the S90 series pictures 4611, 4612, 5175 and 5176. The pictures were imported into a mapping program (Ozi explorer) and the outline and position of surface features could be mapped in UTM coordinates. The new edition of the Norwegian Polar Institute (NPI) 1:100 000 map series of the area was produced from this series, whereas the previous edition was based on the 1936–1938 series.

Unless otherwise stated, the map outlines refer to the 1938 series map whereas the 1995 outline is taken from the 1995 areal phographs.

3.3 Processing

The raw data were processed in ReflexW (2004–2005) and Rad Explorer (2009). The data were checked for gaps and the step sizes were adjusted according to the GPS coordinates. The processing mainly consisted of applying gain (an energy decay function with a scaling factor of 0.6–0.8). The 2010 lines used for amplitude mapping were not subjected to any gain function in order not to bias the amplitude information. All lines were subsequently subjected to background subtraction, DC and a mean subtraction (Dewow) filters. Depending on the noise level and source, or whether horizontal or dipping reflectors were of interest, a subtracting average, running average or band pass filter was applied. Only a few of the lines required migration and a simple diffraction stacking approach was used.

In the 2004–2005 data the bottom reflector was picked and the two way travel time (TWT), depth, amplitude and phase were exported as ASCII files and imported into Petrel. In 2009 and 2010, the lines were depth converted using a velocity of 0,17 m/ns and converted into the standard seg-y format before being imported directly into Petrel. The bottom and surface reflectors were picked and a digital elevation model (DEM) of the area was created by digitizing the NPI 1:100 000 map of the area.

The models were made with a minimum of smoothing while still obtaining reasonable ice thickness contour lines. The resulting 2-D models (Fig. 3) formed the basis for the creation of 3-D models of the surface of the glacier, the bottom reflector (interpreted as the ice-bottom interface) and the terrain of the underlying valley. The bottom reflector can be picked within ± 5 ns corresponding to 0.4 m. A potentially more significant error is the computation of the depth from the TWT. The velocity of pure, cold ice is 0,168 ± 0,003 m/ns (Petterson, 2003). This amounts to an error of 3.5% corresponding to ± 1 m at 30 m depth and ± 3.5 m at 100 m depth.

The underestimation of the ice thickness due to the omission of the effect of the snow layer is very limited and is therefore not taken into account. Snow pits dug on Tellbreen in April of 2009 were 1.2–2.1 m deep, and the snow was found to be hard packed with densities between 340 and 440 g/cm^3. The velocity of radar waves in snow is inversely proportional to the density and therefore not much higher in hard packed snow than in the ice. The velocity in dry firn is 0.19 m/ns (Petterson, 2003) and for hard packed snow 0.22 m/ns. This translates into a time difference in TWT of 5 ns if a 2 m snow layer replaces ice and is equivalent to 0.4 m of ice.

The ice thickness maps and DEMs are not a direct representation of the individual lines but rather an overall smoothed picture of the glacier. The 3 km^2 that are covered by the 2004–2005 lines have 32 700 data points (one per trace). The models have a grid size of 30×30 m which is much larger than the step size (0.5–1.5 m) and 10 times the theoretical coverage as the data points are not evenly distributed on the glacier surface. In 2009, more than 250 000 data point were obtained and again a grid size of 30×30 m was used for the maps of the glacier. A grid of 20×20 m was used for the areas covered by the 2010 data. A comparison between the radar lines from 2005 and 2009 and the two models created from the lines did not show significant differences. However the greatest ice thicknesses were generally underestimated by 3–5 m. This will also influence the bottom topography maps and the average depth and volume estimates. The accuracy of the models based on maps and aerial photos are difficult to quantify since no GPR data exists from before 2004.

The magnitude and polarity of a reflector can give indications of the nature of the interface. The reflection coefficient (R) is a measure for the amount of energy reflected at an interface. Assuming that the conductivity is negligible ($\sigma \approx 0$) it follows that the magnetic permittivity $\mu \approx \mu_0$ when operating at very high frequencies (1 MHz–2 GHz). The relative dielectric permeability of a material (ε_r) is the permittivity of the material ε in relation to the permittivity in free space ε_0. The reflection coefficient can then be expressed as:

$$R = \left(\sqrt{\varepsilon_{r,1}} - \sqrt{\varepsilon_{r,2}}\right) / \left(\sqrt{\varepsilon_{r,1}} + \sqrt{\varepsilon_{r,2}}\right) \text{(Nielsen, 2001)} \quad (2)$$

The index number 1 refers to the material above the interface and 2 the material below. A negative reflection coefficient relates to a shift in polarity of the wave. The reflection coefficients for the most common interfaces found in a glacial environment can generally be divided into two major groups; dry and wet (Fig. 4). Dry interfaces (e.g. ice to shale, air to ice) have reflection coefficients between −0.3 and +0.3 indicating that less than 30% of the incoming wave is reflected back towards the receiving antenna. Wet interfaces (e.g. air to water, ice to wet sand) reflect as much as 80% of the incoming wave and are most often associated with a shift in polarity. An exception to this rule is interfaces where water is the top layer, but as the field work was done in winter this type of interface will be intra or subglacial and therefore overlain by an interface with a $R<0$.

In order to map the properties of the bed of the glacier the relative magnitude, scaled down to [−1;1], and the polarity of the wave at the ice-bed reflection was extracted from the data. This was done using the surface Attribute function in Petrel. The algorithm used was a sum of amplitudes function in a 5ns window centred on the bed reflector (the estimated accuracy to which the reflector could be picked). A contour map of the relative bed reflection amplitude was produced using a grid size of 20×20 m and a minimum curvature algorithm with low grade smoothing. (Fig. 5) This gives an indication of the areas where there are strong indications of a wet interface. When combining (i) the maps of ice thickness and (ii) the locations where structures consistent with subglacial channel are observed in the radar line, this method presents a powerful tool to resolve the origin and transport of the water feeding the icing in front of the glacier.

4 Results

4.1 Temporal changes in geometry, area and volume

To estimate changes to the volume of Tellbreen, four 3-D models of the glacier surface at different times were produced (Table 1 and Fig. 2), based on moraines identified on aerial photographs, map and GPS data. For the 2005 and 2009 models an estimate of both the area of ice visible on areal photos (interpreted as ice with no discernable debris cover in the radar data) and the total ice covered area (where ice thickness was zero) was modelled. The LIA maximum extent of the glacier was approximated by raising the NPI (1936–1939) map surface to the maximum level of the prominent ice-cored moraines that flank the glacier.

At the LIA maximum (approximately 90 years ago; Hodgkins, 1997; Hagen, 2003), the glacier had a volume of 0,47 km^3, compared with 0,42 km^3 in 1936–1938, and less than 0,2 km^3 in 2009. Thus, in a period of less than 100 years since the end of the LIA Tellbreen has lost some 60–70% of its total volume and the glaciated area has been reduced by more than 50%. The long-term mass balance of the glacier (in meter water equivalent per year) was calculated, using the measured surface lowering and an average of the glaciated area, and was found to be -0.6 ± 0.2 m w.e./yr. This figure is close to the -0.55 m/yr that Dowdeswell et al. (1997) gives for Svalbard glaciers as a whole and the findings of Hagen et al. (2003) for valley glaciers of similar size, such as Austre Brøggerbreen (5 km^2, -0.45 ± 0.33 m/yr), Bertilbreen (5 km^2, -0.72 ± 0.29 m/yr) and Longyearbreen (4 km^2, -0.55 ± 0.45 m/yr).

When the GPR data were interpreted it was evident that the bed reflector was generally very clear and distinct, and the overlying ice transparent with few structures. In warm-based polythermal glaciers, there is generally a well defined transition zone from cold ice to ice at the pressure melting point (Hodgkins, 1997; Pälli, 2003), due to the change in water content. In GPR data, this is indicated by a shift from a clear layer with few reflections to a more impenetrable and noisy layer with numerous small reflections. No such change in radar signature was observed on Tellbreen and it is therefore concluded that little, if any, temperate ice exists in the glacier. Support for the idea that Tellbreen is a cold glacier is provided by the low degree of modification and erosion of the valley underlying the glacier, as cold based glaciers have low erosional potential (Etzelmüller, 2000). In a few areas in the upper part of the glacier, complex reflectors occur in the basal zone, interpreted as a 5–15 m thick layer of debris-rich

TCD
4, 2169–2199, 2010

ice. There were also several examples of narrow, inclined structures in the lower part of the glacier which rise downglacier at angles of 5 to 15°. These are interpreted as thrust faults (Fig. 7) The possible presence of both debris-rich ice and thrust faults suggests that the glacier may have been partly warm based at its LIA maximum when parts of the glacier could have been as much as 200 m thick (Fig. 3). This would have encouraged warm-based conditions. There are no indications that Tellbreen has experienced the retreat-advance cycles or subsequent shape changes that are linked to a surge type glacier. The glacier is not currently building up mass in the upper part or undergoing significant increases of surface gradient (Fig. 8). Also there are no indications that the glacier terminus has advanced further into the valley than the LIA extent marked on Fig. 8. The undisturbed and patterned ground in front of the glacier shows no signs of having been glaciated in the last several thousand years, which is the timescale of formation of large-scale patterned ground and ice wedge formation (Mackay, 1990). Taken together with the absence of historical records of the glacier surging, it is concluded that Tellbreen is not of surge type.

4.2 Water in the glacier

Numerous isolated englacial reflectors were observed in the radar data. In the unmigrated data, the structures consist of strong hyperbolas located in otherwise clear ice or just above the bed. These display a reversal of polarity and a reflection pattern consistent with models of air- and partially water-filled englacial channels (Vatne, 2001; Stuart et al., 2003). An englacial channel with a circular or oval cross section will present as a single symmetric hyperbola, whereas a canyon-like morphology (typical of many cut-and-closure type conduits) appears as a series of slightly offset, stacked hyperbolae. More complex reflection patterns can be expected for channels close to the bed, or within debris-rich ice. The polarity and amplitude of the reflected wave is dependent on the reflection coefficients at the interface (Fig. 4).

An example of a structure interpreted to be an englacial channel is shown in Fig. 9. The first arrival from the channel is the reflected R-wave (white-black-white) from the

TCD
4, 2169–2199, 2010

top of the channel. The next arrival is the reversed polarity (black-white-black) TRT-wave that is Transmitted (T) through the ice- air interface at the top of the channel, reflected from the air water interface (R) and transmitted (T) through the air-ice interface. As the reflection coefficient is −0.80 this will result in a high amplitude, reversed polarity signal. The TRRRT-wave is a peg-leg from within the air filled part of the cavity. The TTRTT wave originates from the bottom of the channel (the water-ice interface). The TTRRRTT-wave is again an echo, this time from a peg-leg within the water. Because the propagation velocities of electromagnetic waves in ice, water and air are well established (Annan, 1992), the dimensions of the channel can be estimated. Assuming the channel has a close to circular cross section, the height is ca. 2.3 m, with a water level around 1.5 m. For air-filled channels, the reflection pattern will consequently be simpler. The TRT wave will originate from the bottom of the air-ice interface at the bottom of the channel and the amplitude will be comparatively smaller ($R = -0.28$). The TRRRT-wave can still be observed but not the TTRRRTT-return. For a supraglacial channel (Fig. 10) the general pattern will be the same but the overlying ice will in this case be replaced by a snow bridge with a higher velocity. A subglacial channel can (Fig. 11), due to the low reflection coefficient of ice overlying dry materials, be challenging to detect if no water is present. The reflection pattern of a circular, partly or completely water filled subglacial channel is similar to those of an englacial channel. However, the reflection from the bed of the channel (TRT or TTRTT depending on the water level) will originate from a water-rock/moraine interface with has a lower reflection coefficient than a water-ice interface. Subglacial channels show a large variance in size, shape and geometry, often resulting in a complicated reflection pattern complicating the estimation of geometry and water content.

An analysis of the polarity and strength of the bottom reflector from the 2004, 2005 and 2009 lines showed two areas with high bed reflection power and a distinctly negative reflection coefficient (Fig. 12). One of these areas is near the thickest part of the glacier, and is limited in extent. It is likely that this marks a small, isolated region of wet-based ice. The second, much larger, area occurs beneath the glacier terminus, where the ice is typically less than 20 m thick. The terminus area was investigated in detail in 2010, and the areas with the strongest reflectors and most prominent shift in polarity are highly localized and coincide with structures at or near the bed consistent with a water-bearing channel (Fig. 5). There is no evidence for water at the bed at distances greater than 1 km from the terminus, where the ice is more than 30 m thick. However, englacial reflectors occur above this point, indicative of partially water-filled englacial channels (Fig. 9). Figure 6 is a cross section through the glacier tongue with all channels marked on Fig. 5 plotted as a function of depth and distance to the profile (over or under 50 m). 600–700 m from the terminus the channels are mostly englacial but approaching subglacial. Along the centreline closer to the terminus the majority of the channels are near or at the bed while they are mainly supraglacial near the margins and at the very end tip of the glacier where the ice thickness is below 15 m . This drainage pattern is not consistent with the traditional view of the evolution of drainage systems of cold based glaciers but it is congruent with the recent findings on cold based arctic glaciers (chapter 1).

Subglacial water below the glacier terminus, therefore, appears to be restricted to discrete channels, and there is no evidence for a widespread water film at the bed. In this context, it is relevant that other areas of thin ice around the margins of the glacier are apparently everywhere frozen to the bed (Fig. 7), as is typically the case for Svalbard glaciers. The inferred basal channels do not have any apparent subglacial catchment areas. Instead, it appears likely that they are fed by englacial channels located farther up glacier, which in turn are fed at their upper ends by supraglacial channels.

5 Summary and conclusion

The valley glacier Tellbreen has an area of 4.0 km^2 (1995), the area covered by the radar lines (2009) is 3 km^2. Tellbreen has a volume of 0,15 ± 0.03 km^3, a mean ice thickness of 54 m with a maximum ice thickness of 120 m (2009). It consists of several

TCD
4, 2169–2199, 2010

linked troughs of 80–100 m depth with ridges 20–30 m higher in between. The ridges are highest on the southern side of the valley, lowering towards the middle of the glacier. The topography of the valley underlying the glacier has not been extensively modified by the glacier thus indicating that the glacier has a low erosional potential which is in accordance with the absence of large occurrences of polythermal ice. The valley is mostly V shaped and asymmetrical with steep (30°) walls on the north side, while the slopes on the southern side are only 10°–15°.

Since the end of the LIA, Tellbreen has lost ~60–70% of its volume and the glaciated area has been reduced by more than 50%. The long-term mass balance of the glacier (in meters water equivalent per year) was calculated to be $-0{,}6 \pm 0{,}2$ m w.e./yr. The GPR data indicate that Tellbreen is currently entirely cold-based, with the possible exception of a small, isolated region near the thickest part of the glacier. It is possible that the glacier had more extensive areas of warm-based ice during the LIA maximum, although the low degree of modification of the underlying valley suggests that the glacier has never had high erosional potential. There is no evidence of surge behaviour or an underlying talik.

Despite cold-based conditions, water exits the glacier all year round, and in the winter months feeds a large icing in front of the glacier. Our results indicate that water is stored during the winter months in two or more narrow channels beneath the lowermost 400–500 m of the glacier tongue, from where it is gradually released. These channels are apparently the downglacier continuations of englacial channels, which in turn are fed by supraglacial channels higher up the glacier. This interpretation is consistent with a "cut-and closure" model of drainage system development, in which perennial supraglacial channels progressively incise into the ice, and reach the bed below the thin ice near the glacier terminus. Englacial channels of this type are known to reach cold glacier beds elsewhere in Svalbard. For example, cut-and-closure channels existed at the bed of the cold-based Longyearbreen between 2001 and 2003 (Humlum et al., 2005), although this channel subsequently became blocked and water was rerouted at a higher level within the glacier (Gulley et al., 2009b). Other examples have

TCD
4, 2169–2199, 2010

been observed near the termini of Scott Turnerbreen (Temminghof, 2009) and Rieperbreen (Gulley, unpublished data). Cut-and-closure channels develop where channel incision rates exceed ice surface ablation rates, a process which will tend to bring them into contact with the glacier bed. Channel blockage, however, becomes more likely at greater depths where ice-creep closure rates are higher. This reduces the likelihood that such channels can persist below ice thicker than a few tens of metres. In contrast, cut-and-closure channels could persist below the thin ice near glacier termini, where water could be stored during the winter months.

When seen in connection with the outflow of water from the glacier in winter and the absence of ice at the pressure melting point in the upper part of the glacier, this presents a strong argument for the hypothesis that despite being an entirely cold arctic glacier Tellbreen, contrary to the traditional view of cold based glaciers, has a diverse, subglacial drainage system that is capable of storing, transporting and releasing water year round.

Acknowledgements. Fieldwork was funded by the Norwegian Polar institute Arctic Field Grand and UNIS. We thank M. Riger-Kusk, R. Behlke, Q. Nuna, L. J. Baddeley and U. Silver for their indispensable help during fieldwork.

References

Alley, R. B., Dupont, T. K., Parizek, B. R., and Anandakrishnan, S.: Access of surface meltwater to beds of sub-freezing glaciers: preliminary insights, Ann. Glaciol., 40, 8–14, 2005.

Annan, A. P. and Cosway, S. W.: Ground penetrating radar survey design, Paper prepared for the annual meeting of SAGEEP, Chicago, Sensors & Software, 1992.

Bælum, K.: Mapping of the general shape, depth and various internal structures of Tellbreen, a glacier on Svalbard, by means of GPR. Master Thesis, Aarhus University, Denmark and University Courses of Svalbard, Norway, 2006.

Benn, D. I., Gulley, J., Luckman, A., Adamek, A., and Glowacki, P.: Englacial drainage systems formed by hydrologically driven crevasse propagation, J. Glaciol., 55(191), 513–523, 2009.

Boon, S. and Sharp, M.: The role of hydrologically-driven ice fracture in drainage system evolution on an Arctic glacier, Geophys. Res. Lett., 30(18), 1916-1920, 2003.
Dallmann, W. K., Andresen, A., Bergh, S. G., Harmond Jr, D. M., and Ohta, Y.: Tertiary fold-and-thrust belt of Spitsbergen Svalbard, Norsk Polarinstitut, Oslo, Meddelelser, 128, 1–46, 1993.
Daniels, D. J.: Surface-penetrating radar, Electron Commun Eng., August, 165–182, 1996.
Dowdeswell, J. A., Hagen, J. O., Björnsson, H., Glazovsky, A. F., Harrison, W. D., Holmlund, P., Jania, J., Koerner. R. M., Lefauconnier, B., Simon, C., Ommanney, L., and Thomas, R. H.: The Mass Balance of Circum-Arctic Glaciers and Recent Climate Change, Quaternary Res., 48, 1–14, 1997.
Etzelmüller, B., Ødegård, R. S., Vatne, G., Mysterud, R. S., Tonning, T., and Sollid, J. L.: Glacier characteristics and sediment transfer system of Longyearbreen and Larsbreen, western Spitsbergen, Norsk Geografisk Tidsskrift – Norwegian Journal of Geography, 54(4), 157–168, 2000.
Engeset, R. V. and Ødegård, R. S.: Comparison of annual changes in winter ERS1 SAR images and glacier mass balance of Slakbreen, Svalbard. Int. J. Remote Sens., 20(2), 259–271, 1999.
Fowler, C. M. R.: The Solid Earth. An introduction to global geophysics, Cambridge University Press, Cambridge, UK, 1990.
Gulley, J., Benn, D. I., Screaton, L., and Martin, J.: Englacial conduit formation and implications for subglacial recharge, Quat. Sci. Rev., 28 (19–20), 1984–1999, 2009a.
Gulley, J. D., Benn, D. I., Müller D., and Luckman, A.: A cut-and-closure origin for englacial conduits in uncrevassed regions of polythermal glaciers, J. Glaciol., 55, 189, 66-80, 2009b.
Hagen, J. O., Liestøl, O., Roland, E., and Jørgensen, T.: Glacier atlas of Svalbard, Norsk Polarinstitut, Oslo, Norway, 1993.
Hagen, J. O., Kohler, J., Melvold, K., and Winther, J.-G.: Glaciers in Svalbard: mass balance, runoff and freshwater flux, Polar Res., 22(2), 145–159, 2003.
Hagen, J. O., Melvold, K., Pinglot, F., and Dowdeswell, J.: On the Net Mass Balance of the Glaciers and Ice Caps in Svalbard, Norwegian Arctic. Arct. Antarct Alp. Res., 35(2), 264–270, 2003.
Hansen, O. H.: Internal drainage of some subpolar glaciers on Svalbard, Master thesis, University of Bergen, 2001.
Heincke, B. H., Rønning, J. S., Dalsegg, E., Bælum, K., Wheeler, W., and Nordeide, H. C.:

TCD
4, 2169–2199, 2010

Using 2-D and 3-D georadar to characterize karst collapse as a basis for high-resolution reservoir-analogue models, 12th International Conference on Ground Penetrating Radar, June 16-19, Birmingham, UK, 2008.
Hjelle, A.: Svalbards Geologi., Norsk Polarinstitut, Oslo, Norway, 1993.
Hodgkins, R. Glacier hydrology in Svalbard, Norwegian High Arctic, Quat. Sci. Rev., 16, 957-973, 1997.
Humlum, O., Elberling, B., Hormes, A., Fjordheim, K., Hansen, O. H., and Heinemeier, J.: Late-Holocene glacier growth in Svalbard, documented by subglacial relict vegetation and living soil microbes., Holocene, 15(3), 396–407, 2005.
Humlum, O., Instanes, A., and Sollid, J. L.: Permafrost in Svalbard: a review of research history, climatic background and engineering challenges, Polar Res., 22(2), 191–215, 2003.
Jansson, P., Hock, R., and Schneider, T.: The concept of glacier storage: a review, J. Hydrol., 282, 116–129, 2002.
Liestøl, O.: Glaciological work in 1972, Norsk Polarinstitutt Årbok, 1972, 125–135, 1974.
Mackay, J. R.: Some Observations on the Growth and Deformation of Epigenetic, Syngenetic and Anti-Syngenetic Ice Wedges, Permafrost Periglac., 1, 15–29, 1990.
Neumann, U.: Glacier mass balance investigations in central Spitsbergen 2004 / 2005, Master thesis, University of Oslo, Norway and University Courses of Svalbard, Norway, 2006.
Nielsen, O. F.: Georadar i områder med permafrost, Grønland, Master Thesis, Geofysisk Afdeling, Geologisk Institut, Aarhus Universitet, Danmark, 2001.
Pälli, A.: Polythermal Glacier studies in Svalbard determined by ground penetrating radar, PhD Thesis, Department of Geosciences, University of Oulu, Oulu, Finland, 2003.
Pulina, M.: Norsk Geografisk Tidsskrift – Norwegian Journal of Geography, 38(3,4), 163–168, 1984.
Rachelewicz, G., Szczucinski, W., and Ewertowski, M.: Post- “Little Ice Age” retreat rates of glaciers around Billefjorden in central Spitsbergen, Svalbard. Pol. Polar Res., 28(3), 159–186, 2007.
Riger-Kusk, M.: Hydro chemical and GPS investigations of Longyearbreen, a cold based glacier on Svalbard, Master Thesis, Aarhus University, Denmark and University Courses of Svalbard, Norway, 2006.
Ross, N., Harris, C., Christiansen, H. H., and Brabham, P. J.: Ground penetrating radar investigations of open system pingos, Adventdalen, Svalbard, Norsk Geografisk Tidsskrift, 59, 129–138, 2005.

TCD
4, 2169–2199, 2010

Thermal structure and drainage system of a small valley glacier

K. Bælum and D. I. Benn

Pettersson, R., Jansson. P., and Holmlund. P.: Cold surface layer thinning on Storglaciären, Sweden, observed by repeated ground penetrating radar surveys, J. Geophys Res., 108(F1), 6004–6005, 2003.
Stuart, G., Murray, Y., Gamble, N., Hayes, K., and Hodson, A.: Characterization of englacial channels by ground-penetrating radar: An example from Brøggerbreen, Svalbard. J. Geophys. Res., 108, B11, 2525–2538, 2003.
Sund, M.: A surge of Skobreen, Svalbard. Polar Res., 25(2), 115–122, 2006.
Temminghoff, M.: Characterization of the englacial drainage system in Scott Turnerbreen, Svalbard, by speleological mapping and ground-penetrating radar, Master thesis, University Courses of Svalbard, Norway, 2009.
Turesson, A.: Water content and porosity estimated from ground-penetrating radar and resistivity, J. Appl Geophys, 58, 99–111, 2006.
Vatne, G.: Geometry of englacial water conduits, Austre Brøggerbreen, Svalbard, Norsk Geografisk Tidsskrift – Norwegian Journal of Geography, 55, 85–93, 2001.
Van Hoof, K.: Characterization of englacial conduits in Longyearbreen, Svalbard, by speleological mapping and ground-penetrating radar, Master thesis, University Courses of Svalbard, 2008.
Watts, R. D. and England, A. W.: Radio-echo sounding of temperate glaciers: Ice properties and sounder design criteria: J. Glaciol., 21(85), 39–48, 1976.

Table 1. Volume and areas taken from 3-D models and calculated by Eq. (1). The values are plotted in Fig. 2.

Year		Calculated from Hagen 1993			3-D model	
		Area in km^2	Mean ice thickness in m	Volume in km^3	Mean ice thickness in m	Volume in km^3
1910[a]	LIA maximum	6.4	86	0.55	90	0.48
1938[b]	Map vis. ice	5.8	83	0.48	72	0.42
1977	Glacier atlas	5.4	81	0.44	–	–
1995	vis. ice[c]	3.0	61	0.18	–	–
1995	d_{ice}=0[d]	4.0	71	0.28	–	–
2005	vis. ice[e]	2.6	57	0.15	50	0.13
2005	d_{ice}=0	3.0	61	0.18	50	0.15
2009	vis. ice[e]	2.5	55	0.14	52	0.13
2009	d_{ice}=0	2.8	59	0.17	50	0.14

[a] Estimated from the height and distribution of LIA moraines above the 1995 surface
[b] modelled in Petrel from NP 1:100 000 series map, (based on areal photos from 1936–1938)
[c] Extend of glacier ice on areal photographs
[d] The limits of the ice inferred from the radar lines
[e] Ice with no detectable debris cover in radar lines Average ice thickness d_{ice} = 33 lnA +25 Volume glacier atlas V=A × d

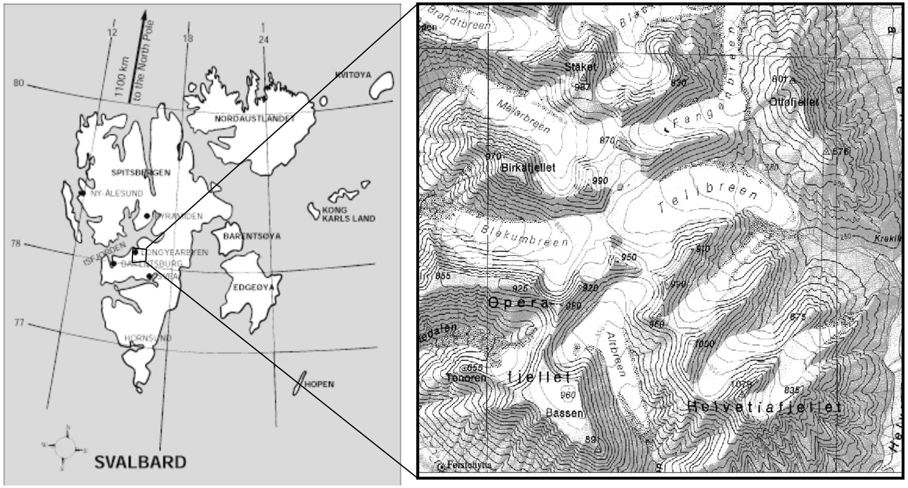

Fig. 1. Location of Tellbreen. The latitudinal positions are in degrees east and the longitudinal positions in degrees north. Map from Norwegian Polar institute.

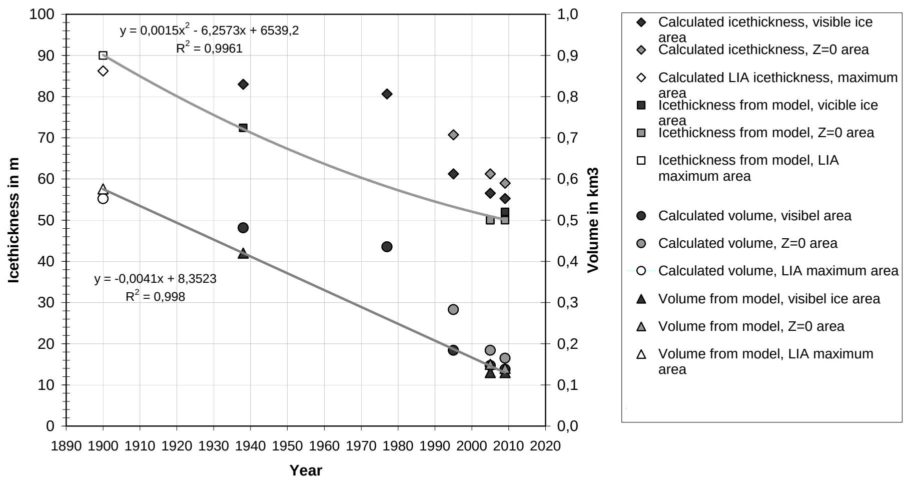

Fig. 2. Plot of and volumes and mean ice thickness of Tellbreen as a function of time. The values can be found in Table 1.

TCD
4, 2169–2199, 2010

Thermal structure and drainage system of a small valley glacier

K. Bælum and D. I. Benn

Title Page
Abstract | Introduction
Conclusions | References
Tables | Figures
Back | Close
Full Screen / Esc
Printer-friendly Version
Interactive Discussion

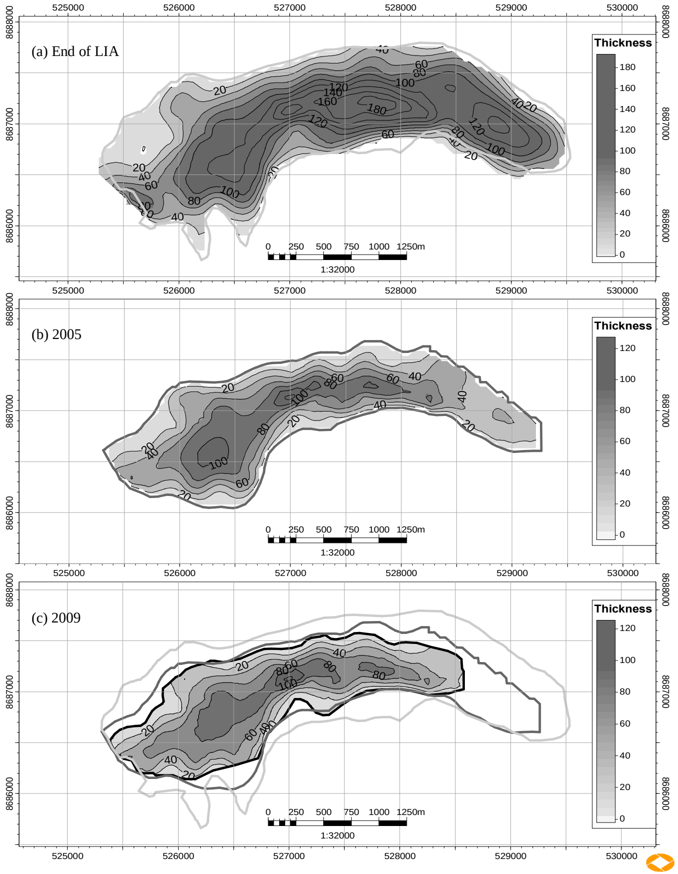

Fig. 3. Ice thickness maps and outlines of the glaciated area. NP 1:100 000 series map (light gray), 2005 measurements (dark grey) and 2009 measurements (black). See the text for the methods used in the calculations.

TCD
4, 2169–2199, 2010

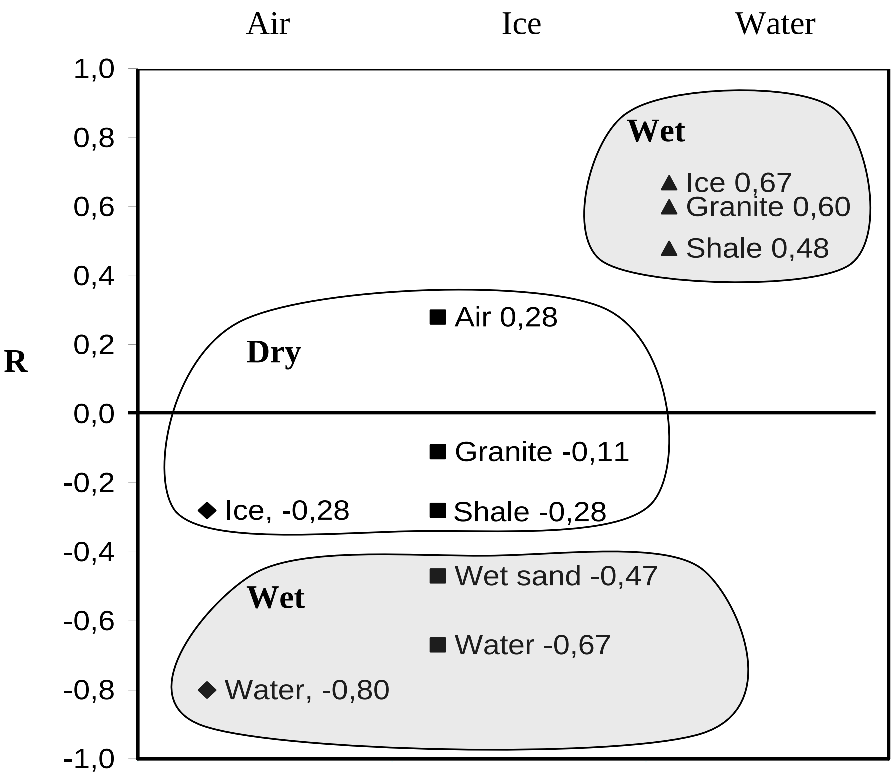

Fig. 4. Reflection coefficients (R) for various interfaces found in a glacial environment. The top caption is the material above the interface; the data labels state the material below the interface and the reflection coefficient. It is clear that the presence of water is connected to a strong reflection.

TCD
4, 2169–2199, 2010

Thermal structure and drainage system of a small valley glacier

K. Bælum and D. I. Benn

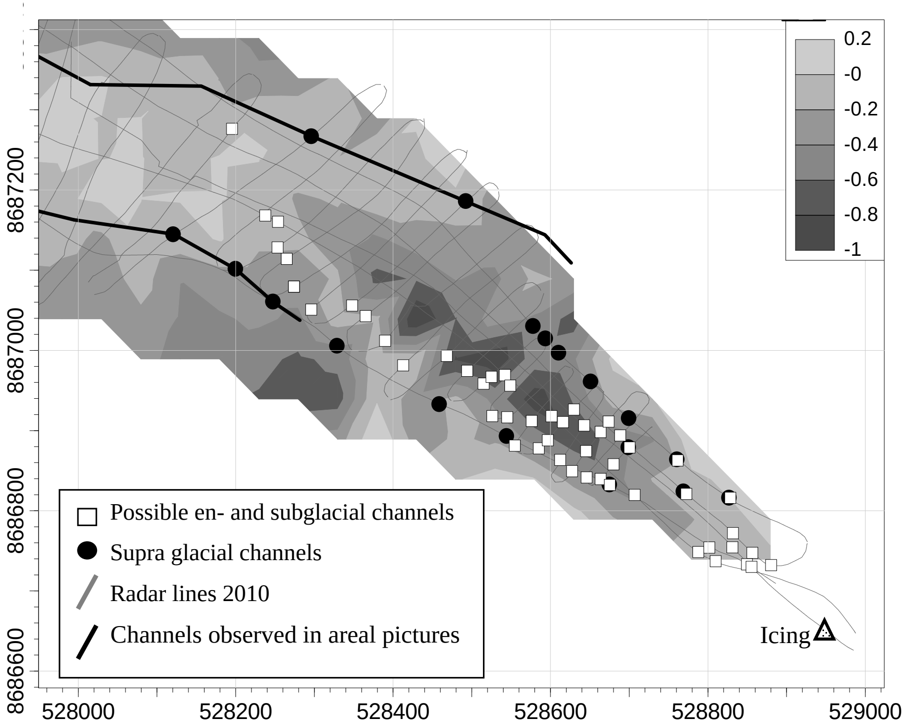

Fig. 5. Relative amplitude of the ice-bed reflector of Tellbreen (2010). The dark areas with values below −0.5, significantly lower than would be expected from a dry interface, are linked to the presence of water at the ice-rock/sediment interface.

TCD
4, 2169–2199, 2010

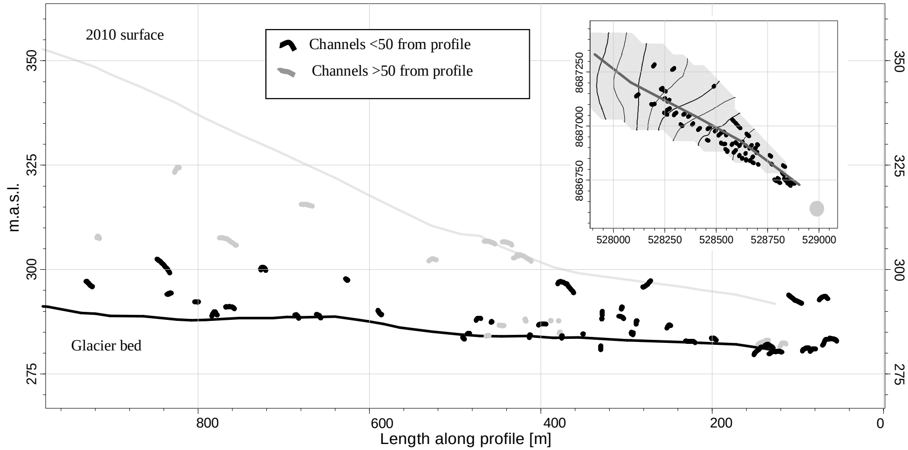

Fig. 6. Cross-section of terminus with all channels identified in the 2010 lines plotted in map view (small inset) and as a function of depth and length along the profile. The channels are coloured according to distance from profile line.

TCD
4, 2169–2199, 2010

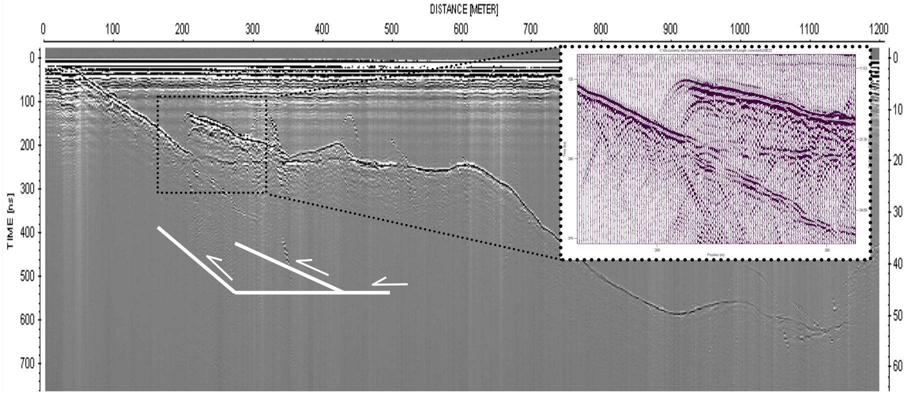

Fig. 7. A thrust fault near the terminus of the glacier. Detail from line running from the terminus up the centre of the glacier. Top and right hand scales are in m, left hand is TWT in ns. Notice the 600 m of ice that is less than 20 m thick. Gain and dewow are applied.

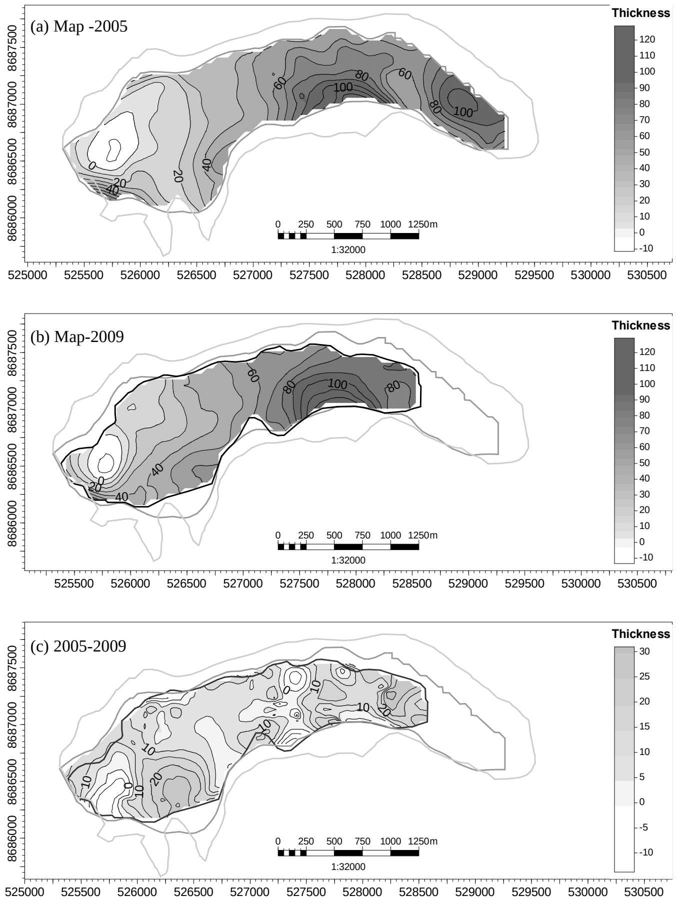

Fig. 8. The change in surface elevation and outline of Tellbreen. Norwegian Polar Institute A7 map, 1:100 000 series outline (Light grey). 2005 area covered by GPS measurements (Dark grey) and 2009 area covered DGPS measurements (black).

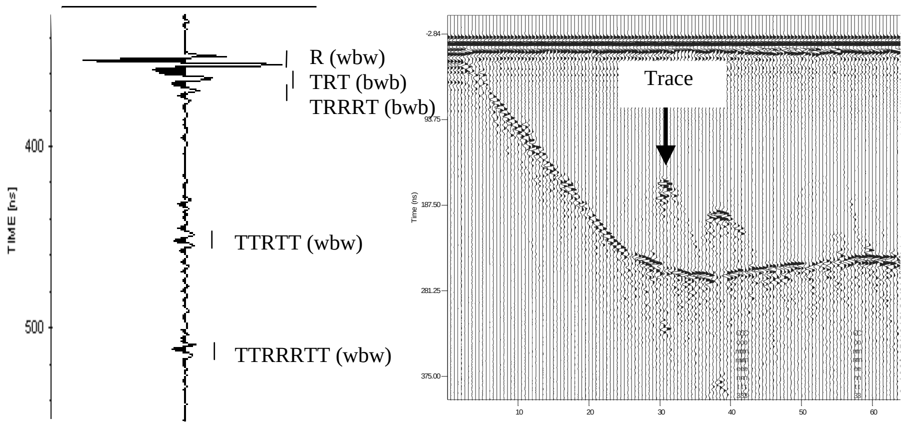

Fig. 9. Wavelet trace of an englacial channel. Detail from a cross glacier line. The radar signature can be interpreted as a 2/3 water filled englacial channel ca. 2.3 m in diameter.

TCD
4, 2169–2199, 2010

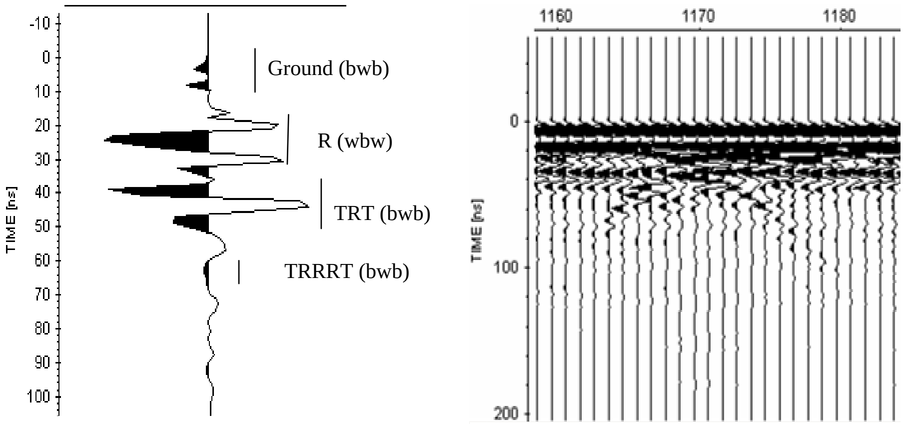

Fig. 10. Wavelet trace of a 2–4 m deep, lateral melt water channel. The curvature of the hyperbola indicates a velocity of around 0.22 m/ns as a reasonable value for a snow filled channel.

TCD
4, 2169–2199, 2010

Thermal structure and drainage system of a small valley glacier

K. Bælum and D. I. Benn

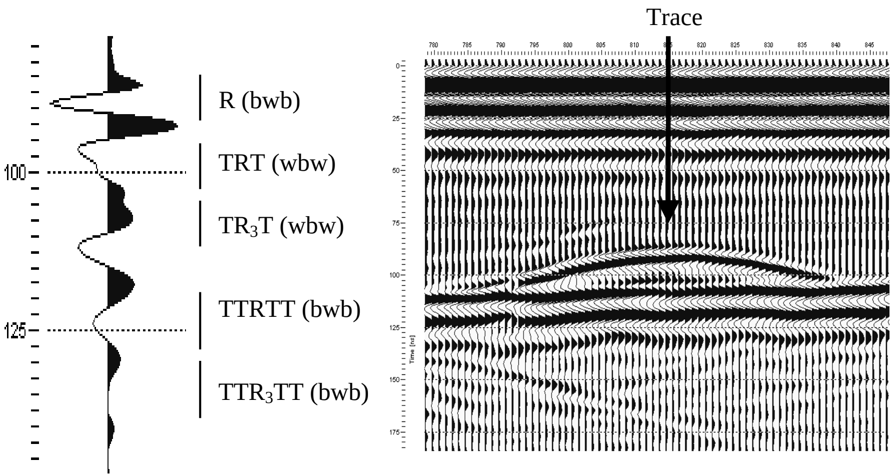

Fig. 11. Partially water filled subglacial channel near the terminus. The top hyperbola collapses with a migration velocity of velocity of 0.29 m/ns. The channel is ca 2 m high with 0.5 m of water.

TCD
4, 2169–2199, 2010

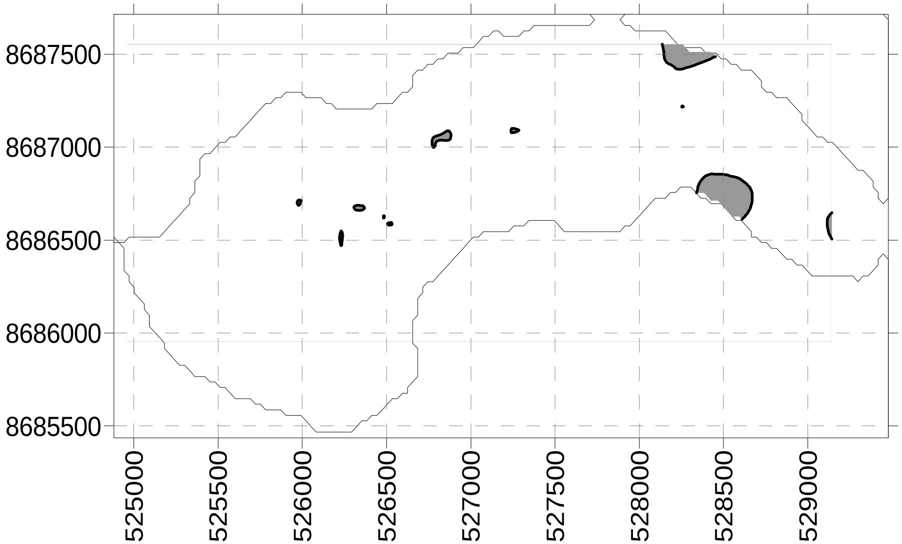

Fig. 12. Map of areas (2009) where the relative amplitude of the ice-bed reflector is below −0.5. These areas are assumed to be related to the presence of water at the interface and temperate ice. Outline of glacier from the Norwegian Polar Institute map.